Supporting Information

Title Spatiotemporally programmable metasurfaces via viscoelastic shell snapping

*Yuzhen Chen, Tianzhen Liu, and Lihua Jin**

Supplementary Text 1: Material modeling and characterization

We used the following incompressible neo-Hookean material model to define the instantaneous constitutive behavior of the shells,

$$W = \frac{\mu}{2}\left[\mathrm{tr}\left(\mathbf{F}\mathbf{F}^{\mathrm{T}}\right) - 3\right], \tag{S1}$$

where W is the strain energy density function, μ is the shear modulus, $\mathbf{F}$ is the deformation gradient tensor. To describe the viscoelastic behavior of the shells, Prony series were used and the shear modulus μ can be expressed as

$$\mu(t) = \mu_0\left[1 - \sum_{i=1}^{n} g_i\left(1 - e^{-t/\tau_i}\right)\right], \tag{S2}$$

where μ_0 is the instantaneous shear modulus, n is the number of the series terms, g_i is the dimensionless relaxation modulus, t is the time, and τ_i is the relaxation time constant.

Here we characterize the viscoelastic properties of the silicone rubber (Dragon SkinTM30) and urethane rubber (VytaFlexTM 20)**.** We modeled their viscous part as two-term Prony series (n = 2 in Eq. S2). Combining Eq. S1 and S2, the nominal (first Piola-Kirchoff) stress under uniaxial tension is then given by

$$S_{11} = \mu(t)\left(\lambda - 1/\lambda^2\right), \tag{S3}$$

where S_{11} and λ represent the nominal stress and stretch along the loading direction, respectively, $\mu(t)$ is the shear modulus at time t,

$$\mu(t) = \mu_0\left[1 - g_1\left(1 - e^{-t/\tau_1}\right) - g_2\left(1 - e^{-t/\tau_2}\right)\right]. \quad \text{(S4)}$$

During the stress relaxation tests, λ =1.2 was applied instantaneously, and S_{11} decaying as a function of time was measured. Substituting the measured S_{11} into Eq. S3 to obtain the $\mu - t$ relation, and fitting Eq. S4 to the experimental data using the linear least-square method, we obtained μ_0, g_1, τ_1, g_2, τ_2 for the two materials, as shown in Table 1. In Figure S1, we can see that the two-term Prony series are sufficient for an accurate fit (the root-mean-square error is less than 0.6%).

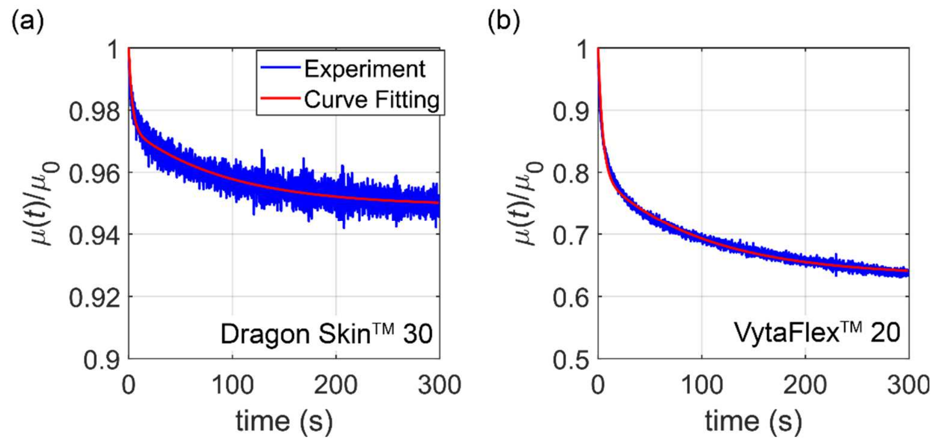

Figure S1. Characterization of the viscoelastic properties for the silicone rubber (Dragon Skin™30) and urethane rubber (VytaFlex™ 20). (a-b) The evolution of the normalized shear modulus over time, $\mu(t)$, during the stress relaxation tests for Dragon Skin™ 30 (a) and VytaFlex™ 20 (b). The blue curves represent the experimental data, while the red curves represent the curve fitting.

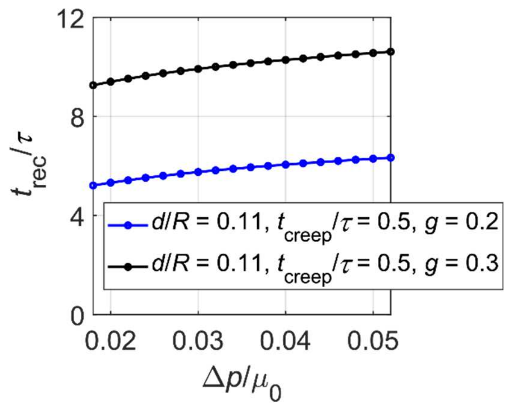

Figure S2. Pressure $\Delta p/\mu_0$ has a small effect on the recovery time t_{rec}/τ. The shells with H/R = 0.4, d/R = 0.11, g = 0.2 (blue curve) or 0.3 (black curve) are subjected to a constant pressure $\Delta p/\mu_0$ for t_{creep}/τ = 0.5 prior to its releasing. As $\Delta p/\mu_0$ increases from 0.02 to 0.05, t_{rec}/τ only increases by 18.20% (g = 0.2) and 12.34% (g = 0.3).

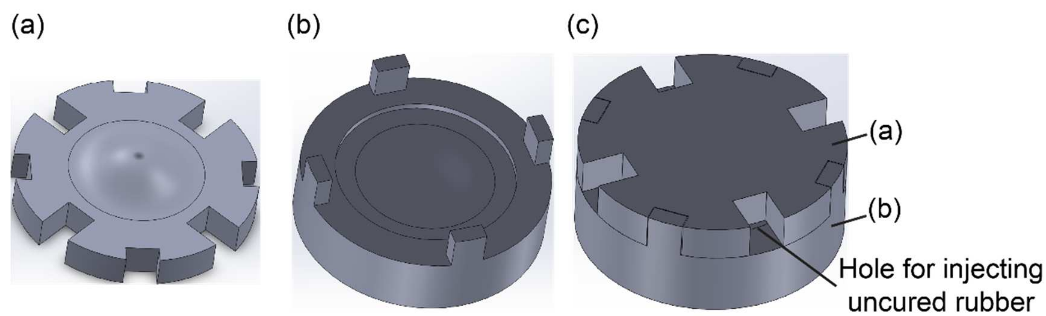

Figure S3. The 3D model of the two-part mold for fabricating viscoelastic shells. This mold (c) consists of the upper part (a) and lower part (b). The uncured rubber is injected into the mold through any one of the four holes on the mold.

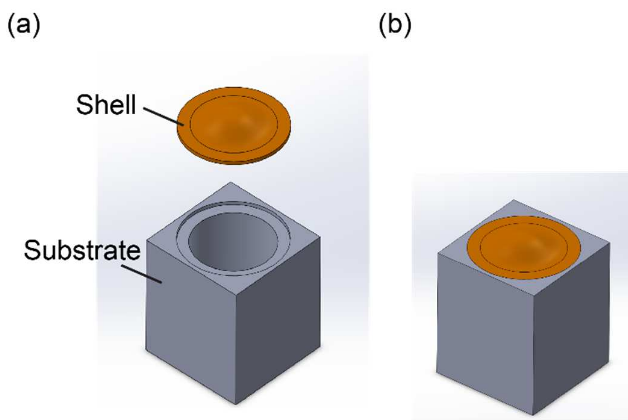

Figure S4. The assembly of the shell and the substrate. (a) The 3D model of the substrate. The substrate has a cylindrical chamber with radius 10 mm and height 34 mm. It also has a step structure with the same width (3 mm) as the flange of the shell. (b) The shell is bonded onto the substrate by applying super glues onto its flange. The step structure on the substrate can guarantee the concentricity between the shell and the substrate.

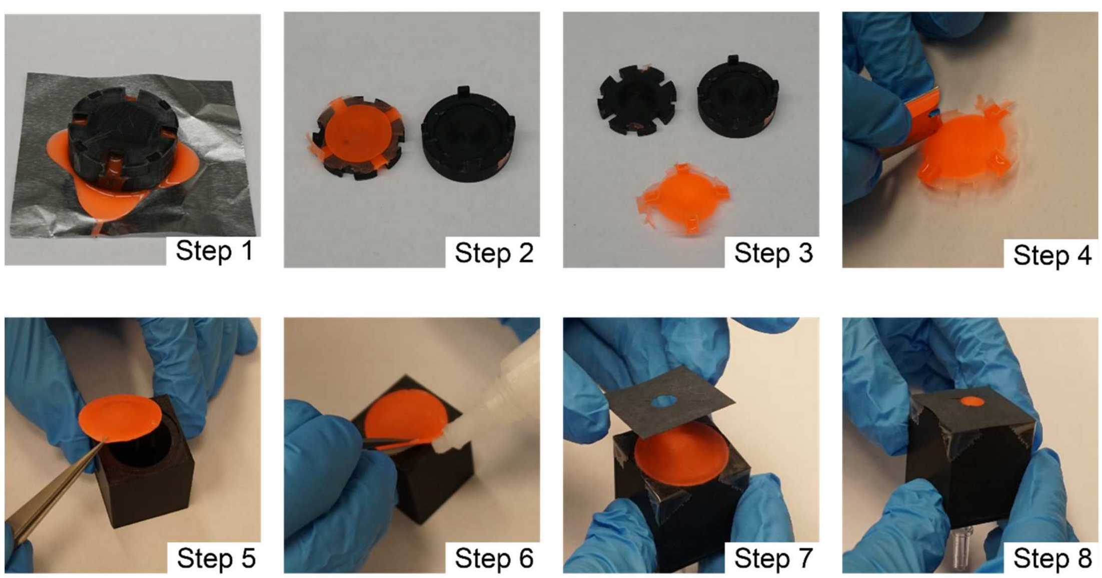

Figure S5. The fabrication procedure of a shell unit. Step 1, inject uncured rubber into the mold through the holes on the mold using syringes. Step 2, open the mold after the rubber is fully cured. Step 3, peel off the shell. Step 4, cut the excessive parts from the shell. Step 5, place and align the shell on the top of the hollow substrate. Step 6, glue the flange part of the shell onto the substrate. Step 7, when needed, align a flexible black paper with a hole at its center with the shell. Step 8, bond the paper on the substrate via double-sided tapes.

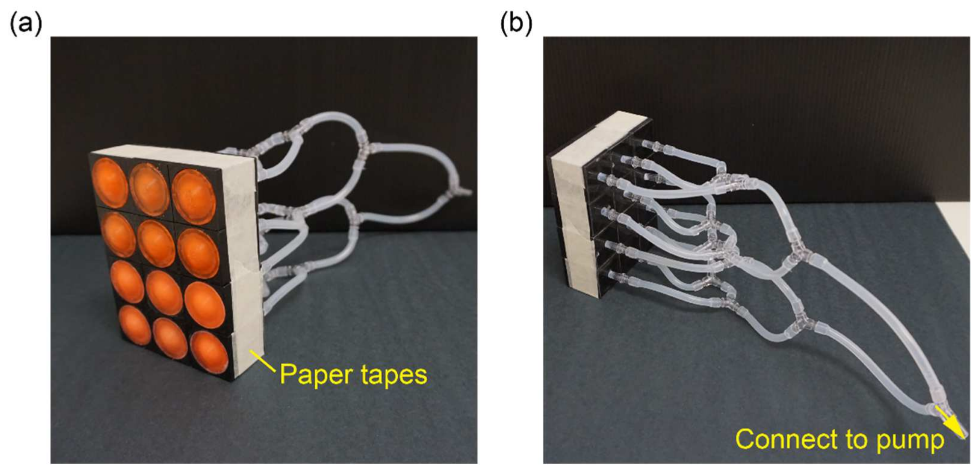

Figure S6. Metasurface and its tubing. (a) Oblique view of the metasurface. The metasurface is created by aligning and binding the shell units together by paper tapes. (b) Back view of the metasurface. The shell units are interconnected via silicone tubing in a way that the shell units have equal distances to the vacuum pump.

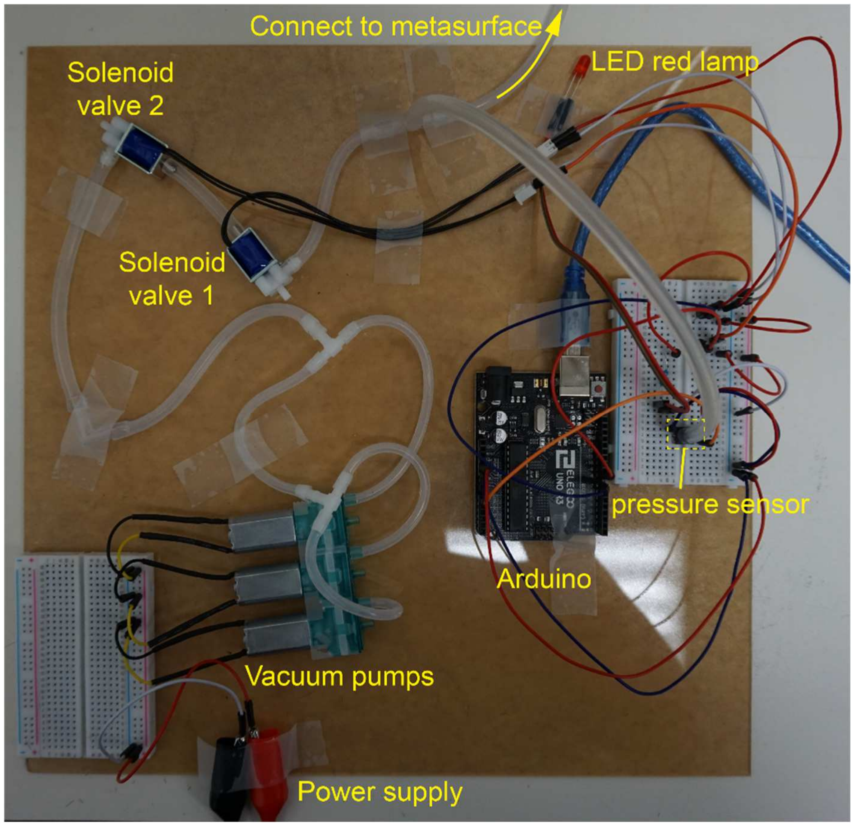

Figure S7. Pneumatic actuation system used to control the pressure loading history.

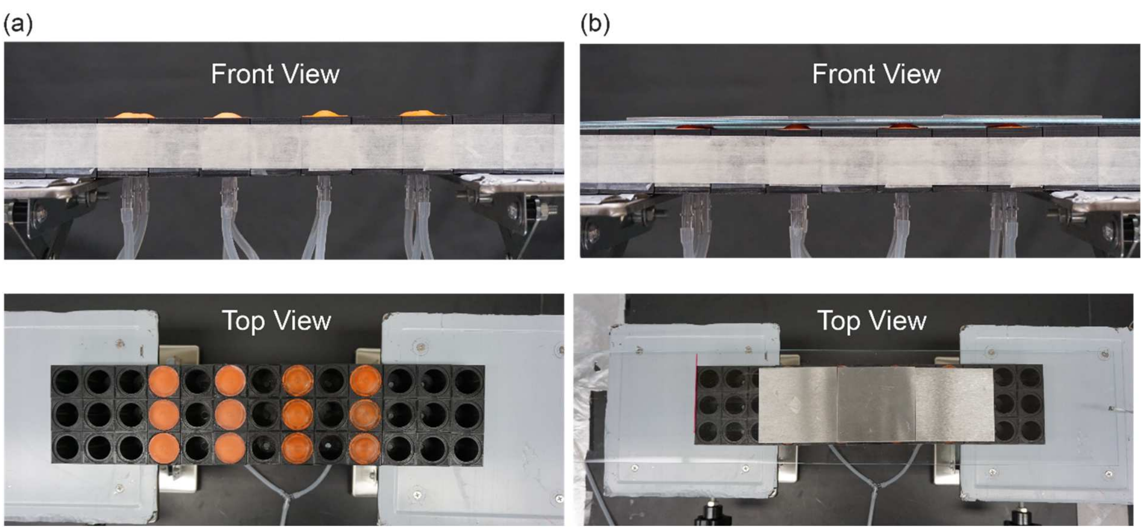

Figure S8. Experimental setup for measuring the effective frictional coefficients between an acrylic board and a metasurface. (a) Front and top view of a metasurface with a mixture of the four types of shell units. From left to right: bistable shell units, the shell units with zero, medium, and long recovery time. (b) Front and top view of the metasurface when an acrylic board together with a weight is placed on it.

Movie S1. Metasurface composed of viscoelastic shells with different recovery time in each row

Movie S2. Metasurface displaying temporal evolution of digit numbers

Movie S3. Metasurface displaying temporal evolution of emoji